Applied Physics Letters ARTICLE scitation.org/journal/apl

On-demand cold plasma activation of acetyl donors for bacteria and virus decontamination

Cite as: Appl. Phys. Lett. **119**, 054104 (2021); doi: 10.1063/5.0062787
Submitted: 8 July 2021 · Accepted: 27 July 2021 ·
Published Online: 5 August 2021

Endre J. Szili,[1,a] Bhagirath Ghimire,[2] Bethany Lee Patenall,[3] Mohammed Rohaim,[4] Dharmit Mistry,[5] Adrian Fellows,[5] Muhammad Munir,[4] A. Toby A. Jenkins,[3] and Robert D. Short[1,2,a]

AFFILIATIONS

[1]Future Industries Institute, University of South Australia, Adelaide SA 5095, Australia
[2]Department of Chemistry and Material Science Institute, Lancaster LA1 4YB, United Kingdom
[3]Department of Chemistry, University of Bath, Bath BA2 7AY, United Kingdom
[4]Division of Biomedical and Life Sciences, Lancaster University, Lancaster LA1 4YW, United Kingdom
[5]AGA Nanotech Ltd., 2 Regal Way, Watford, Hertfordshire WD24 4YJ, United Kingdom

[a]**Authors to whom correspondence should be addressed:** endre.szili@unisa.edu.au and r.d.short1@lancaster.ac.uk

ABSTRACT

Antibiotics are commonly used as the first line of defense in the treatment of infectious diseases. However, the rise of antimicrobial resistance (AMR) is rendering many antibiotics less effective. Consequently, effective non-antibiotic antimicrobial strategies are urgently needed to combat AMR. This paper presents a strategy utilizing cold plasma for the "on-demand" activation of acetyl donor molecules. The process generates an aqueous-based antimicrobial formulation comprising a rich mixture of highly oxidizing molecules: peracetic acid, hydrogen peroxide, and other reactive oxygen and nitrogen species. The synergistic potent oxidative action between these molecules is shown to be highly effective at eradicating common wound pathogenic bacteria (*Pseudomonas aeruginosa* and *Staphylococcus aureus*) and at inactivating a virus (SARS-CoV-2).

Antimicrobials are the most widely used therapeutic drugs worldwide. They have revolutionized medicine, farming and agriculture, and veterinary care and are used in many other industries, including commercial paint formulations. However, their overuse, particularly in the case of antibiotics, has rendered them less effective through the rise of antimicrobial resistance (AMR).[1] By 2050, AMR is forecasted to cause 10M deaths per annum resulting in a potential US$100 trillion shock to the global economy.[2] Consequently, there is a need for on demand antibiotic-free solutions for microbial eradication to eliminate the growing problem of AMR in healthcare and in our environment.

This study describes an antibiotic-free strategy utilizing the cold plasma activation of acetyl donor antimicrobial precursors. The process generates a potent antimicrobial water-based disinfectant (Fig. 1). Cold plasma is a low-temperature (e.g., human tissue tolerable) electrically generated partially ionized glow-discharge. When operated into air, cold plasma activates the surrounding oxygen, nitrogen, and water vapor molecules, generating reactive oxygen and nitrogen species (RONS).[3–7] These RONS can oxidize molecules and cells, which is potentially useful for a broad range of applications, including water purification, sterilization, and decontamination of pathogenic microorganisms.[8] Some of these RONS have a high Henry's law constant, such as hydrogen peroxide (H_2O_2) = 1.92×10^6 and peroxynitrous acid (ONOOH) = 4.8×10^6, allowing them to be easily solubilized when delivered by cold plasma into aqueous solutions (e.g., water).[9] In combination, H_2O_2 and ONOOH can kill microorganisms through oxidative stress, exacerbated at low pH.[10–12] However, many microorganisms have efficient antioxidant defense mechanisms that reduce the antimicrobial efficacy of cold plasma, including certain pathogenic bacteria, which can release catalase—an antioxidant enzyme that neutralizes H_2O_2.[13] To mitigate this likely problem, we investigated the use of two antimicrobial precursor acetyl donors, tetraacetylethylenediamine (TAED) and pentaacetate glucose (PAG), to amplify the antimicrobial effects of cold plasma. TAED and PAG and their by-products are readily biodegradable and are nontoxic if used at low concentrations and can be manufactured using green chemistry.[14–16] Plasma generated H_2O_2 reacts with the acetyl donors of TAED and PAG to produce peracetic acid (PAA), which acts in synergy with H_2O_2 and other plasma generated RONS, providing a potent broad-spectrum antimicrobial solution (Fig. 1). PAA at the low concentration used in this study has been shown to be nontoxic in an

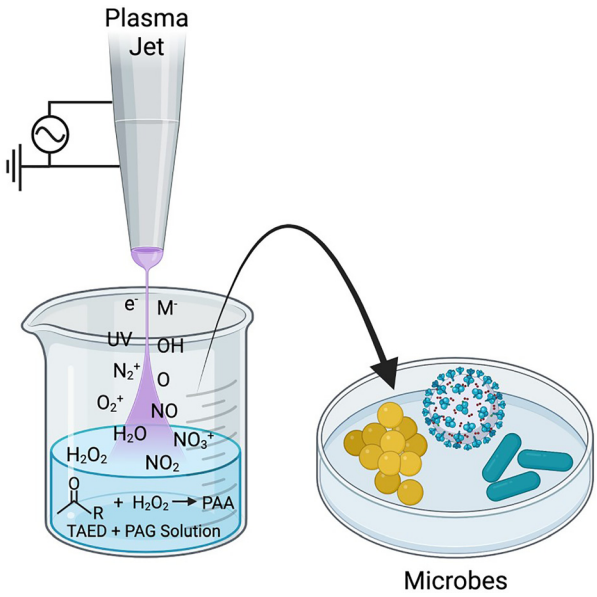

FIG. 1. Pictorial overview of the cold plasma activation of an acetyl donor from TAED and PAG generating PAA, H_2O_2, and other RONS for the eradication of pathogenic microbes.

animal model.[15] Furthermore, PAA does not easily give rise to AMR[15] and is used in many industrial applications, including food decontamination,[17] wastewater treatment,[18] hospital waste sterilization,[19] and medical instrument disinfection.[20] An advantage of PAA for these applications is that it does not leave harmful residues as it quickly decomposes to acetic acid, oxygen, and water.

The cold plasma jet used for these experiments consisted of an internal stainless steel pin high voltage (HV) electrode sealed inside a quartz tube [inner diameter (ID) = 1.5 mm, outer diameter (OD) = 3 mm]. Two cylindrical ground electrodes made up of copper were placed at positions of 56 and 110 mm below the tip of the HV electrode [Fig. 2(a)]. The first ground electrode helped to reduce the breakdown voltage, while the second ground electrode served to increase the length of the plasma jet. The tube length of 164 mm below the HV electrode was designed to maximize the production of H_2O_2.[21] Plasma was ignited by purging the Ar gas at 1 standard liters per minute through the tube and supplying 2.38 kV rms voltage at 23.5 kHz to the HV electrode producing a dissipated power of 2.71 W [Fig. 2(b), also see supplementary material S1]. Under the prescribed conditions, a plasma jet extends out of the tube to a distance of ~14 mm [Fig. 2(a)] with an optical emission typical of highly reactive species that form RONS through downstream reactions [Fig. 2(c) and supplementary material S2]. The average gas temperature (T_g) of the plasma jet (measured with an infrared thermometer, Fluke 62 Max) was found to be cool at 310.5 ± 3.5 K at 4 mm position outside of the tube's orifice (i.e., at the same position as the liquid targets). Optical

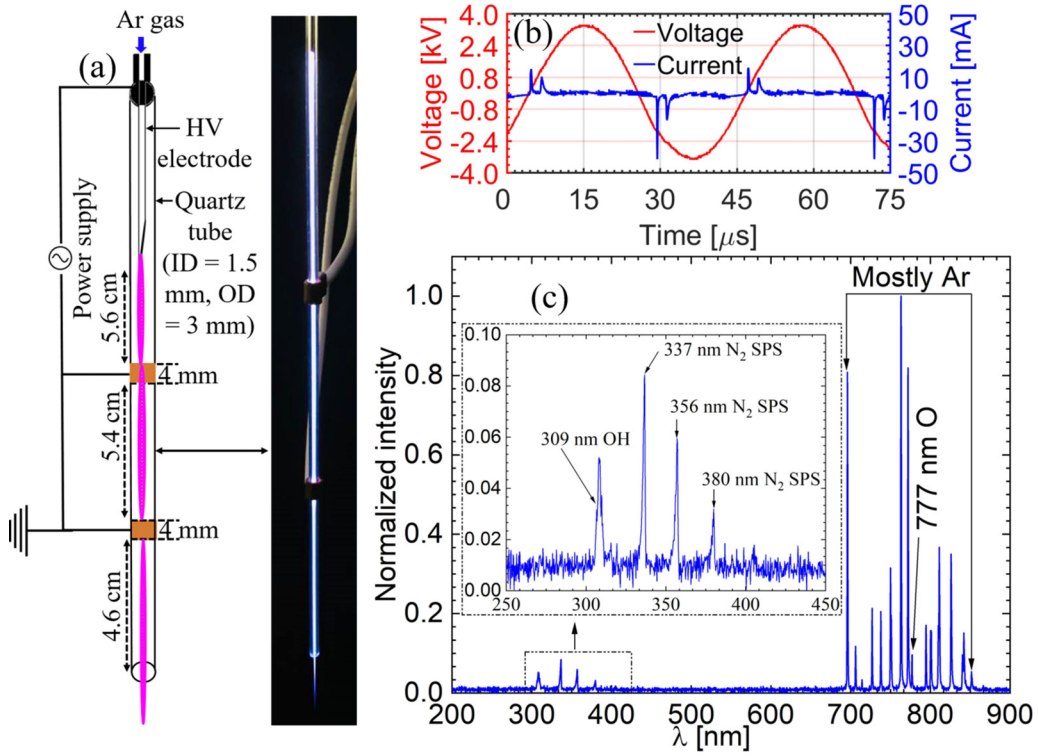

FIG. 2. (a) Setup of the cold plasma jet assembly, (b) its current–voltage waveforms, and (c) optical emission spectra of the plasma discharge.

emission spectra shown in Fig. 2(c) were used to estimate the electron temperature (T_e) and vibrational temperature (T_v) of the plasma jet. T_e was calculated using the collisional-radiative model,[22] while T_v was derived from the Boltzmann plot by analyzing the spectral bands of the nitrogen second positive system.[23] The values of T_e and T_v for the plasma jet were found to be 0.73 eV and 2323 K, respectively. A high value of electron temperature as compared to relatively low values of ion and neutral gas temperature (i.e., $T_e \gg T_v \gg T_g$) verifies the non-thermal characteristics of the plasma jet. A mixture of 2.5 mM TAED with 2.5 mM PAG in 350 μl de-ionized water (DIW) was used as the antimicrobial precursor because this blended system was previously shown to produce the optimal antimicrobial efficacy compared to the molecules used alone.[24] The antimicrobial efficacy of the plasma activated TAED-PAG (PA-TP) was compared to plasma activated DIW (PA-DIW) produced under the same plasma conditions. Statistical analysis was performed using a two-sample student *t*-test of unequal variance considering a $p < 0.05$ as significant.

The major longer-lived antibacterial agents in PA-TP are H_2O_2 and PAA. Figure 3 (and supplementary material S3) shows that the concentration of H_2O_2 and PAA in PA-TP was 4.5 and 2.9 mM, respectively. PA-DIW had a slightly lower H_2O_2 concentration at 2.5 mM and contained no PAA because of the absence of TAED and PAG. PA-TP was more acidic at pH 2 compared to PA-DIW at pH 4.

Formation of H_2O_2 in PA-DIW and PA-TP is known to occur through several pathways. This mainly occurs through the formation of an intermittent product (hydroxyl radical, $^{\bullet}OH$) through:[5,21,22]

(a) collisions with electrons: e- + $H_2O \rightarrow H + {}^{\bullet}OH + e^-$,
(b) collisions with metastable atoms/radicals: $e^- + O_2 \rightarrow O(^3P) + O(^1D) + e^-$, $O(^1D) + H_2O \rightarrow 2{}^{\bullet}OH$; $e^- + N_2 \rightarrow N_2(A^3\Sigma_u^+) + e^-$, $N_2(A^3\Sigma_u^+) + H_2O \rightarrow {}^{\bullet}OH + N_2 + H$,
(c) collisions with argon metastables: $e^- + Ar \rightarrow Ar_m + e^-$, $Ar_m + H_2O \rightarrow Ar + H_2O^+ + e^-$; $e^- + H_2O+ \rightarrow {}^{\bullet}OH + H$,
(d) plasma initiated ultra-violet (UV) photolysis: $UV + H_2O \rightarrow H_2O^*$; $UV + H_2O^* \rightarrow H^+ + OH^-$; $OH^- \rightarrow {}^{\bullet}OH + e^-$.

$^{\bullet}OH$ radicals formed through (a)–(d) subsequently recombine to form H_2O_2 as shown in the reaction: $^{\bullet}OH + {}^{\bullet}OH \rightarrow H_2O_2$. The plasma generated H_2O_2 molecules subsequently react with the acetyl donor-containing molecules to form PAA.

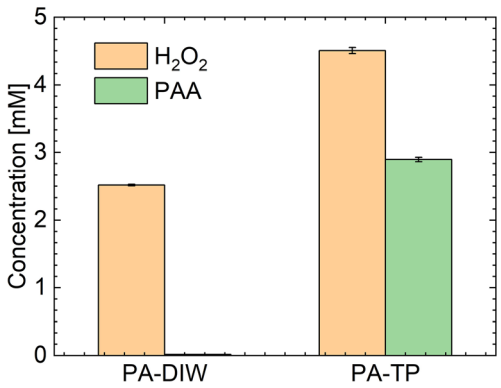

FIG. 3. Concentration of H_2O_2 and PAA in the PA-DIW and PA-TP.

In the next experiments, the oxidizing capacity of PA-TP and PA-DIW compared to standard H_2O_2 solutions was tested through their ability to oxidize potassium iodide (KI, supplementary material S3). The principle is based upon the oxidation of KI to produce triiodide ions with an absorbance maximum of 350 nm. TAED-PAG alone (i.e., prior to plasma activation) produces zero absorbance reading at 350 nm, indicating that it does not oxidize KI (due to the absence of oxidants). Figure 4 shows that 0.61–10 mM H_2O_2 solutions readily oxidize KI. A statistically identical level of KI oxidation was achieved with 2.5–5 mM H_2O_2 ($p > 0.05$), indicating that the small differences in the H_2O_2 concentrations in PA-TP (4.5 mM) and PA-DIW (2.9 mM) should not be a major contributing factor to their oxidative capacity. A slightly higher level of KI oxidation was produced by PA-DIW (absorbance at 350 nm = 0.5) compared to the equivalent 2.5 mM H_2O_2 standard solution (absorbance at 350 nm = 0.37). This result is attributed to other RONS in the PA-DIW making a further small contribution to the oxidation of KI. PA-TP produced a significantly higher level of oxidized KI (absorbance at 350 nm = 2.4) compared to PA-DIW ($p < 0.05$) attributed to the synergistic oxidation of KI by PAA, H_2O_2, and other RONS.

The presence of 75 mg/ml catalase abolished the oxidative capacity of the standard H_2O_2 solutions and PA-DIW (Fig. 4). This indicates that H_2O_2 was the major oxidant in PA-DIW. Conversely, catalase did not abrogate the oxidative capacity of PA-TP (absorbance at 350 nm = 0.5). This result is attributed to the additional oxidant PAA (in PA-TP) that is not affected by the catalase.

Finally, the antimicrobial property of PA-TP and PA-DIW was assessed (supplementary material S4). First assessment was carried out by examining their bactericidal action against common wound pathogens Gram-negative *Pseudomonas aeruginosa (P. aeruginosa)* and *Gram-positive Staphylococcus aureus (S. aureus)* in the planktonic state. Optical density (OD) measurement of the bacteria broth was used to assess bacterial growth. Figure 5(a) shows that the final OD measured in the *P. aeruginosa* culture following treatment with the PA-DIW was lower compared to the untreated bacteria positive control ($p < 0.05$) and the same as the sterile broth negative control ($p > 0.05$), indicating that PA-DIW significantly reduced the growth of the bacteria. However, PA-DIW was not bactericidal against *S.*

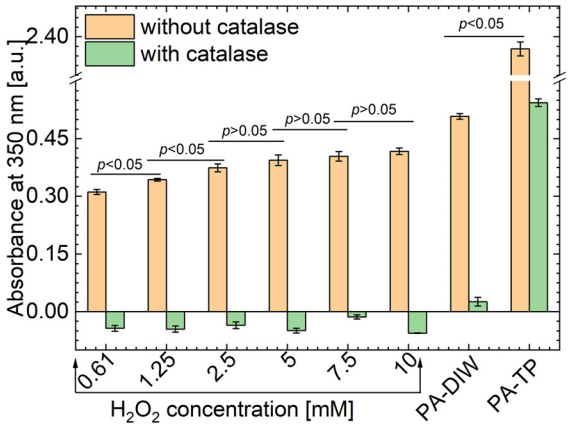

FIG. 4. Oxidation of KI from varying concentrations of H_2O_2, PA-DIW, and PA-TP with and without the presence of catalase.

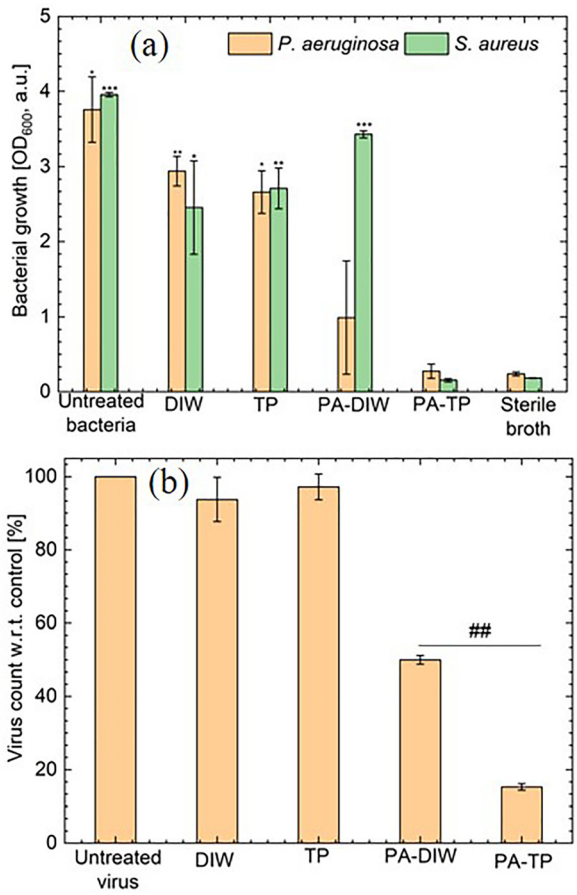

FIG. 5. (a) Reduction in growth of *P. aeruginosa* and *S. aureus* by PA-DIW and PA-TP. Results were compared to untreated DIW and TP solutions. Positive control = Untreated bacteria; Negative control = Sterile broth. Following treatment, bacteria were incubated in the test solutions for 18 h. (b) Reduction in SARS-CoV-2 viral load by PA-DIW and PA-TP. Results were compared to untreated DIW and TP solutions and untreated virus as a positive control. The asterisk (∗) symbols above the bars in 5(a) represent statistical significance compared to sterile broth (bacteria) with one symbol $p = 0.01$–0.05, two symbols $p = 0.001$–0.01, and three symbols $p < 0.001$. The # above PA-TP in 5(b) represents a statistical significance of $p < 0.05$ compared to PA-DIW.

aureus [Fig. 5(a)], presumably due to its more complex Gram-positive membrane structure providing a barrier against the treatment. In comparison, PA-TP treatments decreased bacterial load for *P. aeruginosa* and *S. aureus* to an undetectable level ($p > 0.05$ compared to the sterile broth). These results indicate that PA-TP is a more effective bactericidal agent compared to PA-DIW. Based on our protocols, the starting culture of 2×10^6 CFU/ml used in this assay (supplementary material S4) would equate to $\sim 10^9$ CFU/ml, corresponding to an OD of ~4 for both bacteria. Therefore, we estimate that the results achieved with the PA-TP correspond to at least a 10^6-log up to a maximum of $\sim 10^9$-log reduction in bacterial growth. Similar trends were observed when the virucidal activities of PA-TP and PA-DIW were tested against SARS-CoV-2 (supplementary material S5). Figure 5(b) shows that the PA-DIW reduced the viral load by 50%, whereas PA-TP achieved a greater reduction in viral load of >84%. Importantly, neither the DIW nor the TP solutions alone (i.e., without plasma activation) were antimicrobial against the bacteria and the virus in Figs. 5(a) and 5(b). This shows that the high antimicrobial activity of PA-TP is indeed attributed to the unique combination of the cold plasma jet treatment with TP, which is activated on-demand upon plasma ignition. The test solutions used in Fig. 5 were diluted fourfold (supplementary material S5), and this was kept constant for both bacteria and virus assays. We anticipate that a more concentrate PA-TP solution would yield a higher level of virus inactivation.

Overall, this study demonstrates how the antimicrobial effects of cold plasma can be amplified with acetyl donor molecules. The acetyl donor formulation can be configured for on-demand use either in a liquid formulation as demonstrated in this study or potentially in a cream or gel formulation or even within a hydrogel wound dressing activated by a small hand-held cold plasma device. Major advantages of on-demand PA-TP for these applications include the ability to produce stable formulations with a long shelf-life and without the requirement of refrigeration, and its multipronged action coupled with on-demand activation prevents prolonged exposure of microorganisms to sub-optimal concentrations of the antibacterial agents; all of which are likely to help resist the development of AMR in healthcare and in our environment.

See the supplementary material for measurement and calculation of cold plasma jet dissipated power (supplementary material 1), optical emission spectrum from the cold plasma jet (supplementary material 2), measurement of H_2O_2 and PAA after cold plasma activation of DIW/acetyl donors (supplementary material 3), antibacterial assays (supplementary material 4), and antiviral assays (supplementary material 5).

AUTHORS' CONTRIBUTIONS

E.J.S. and B.G. contributed equally to this work.

The authors would like to thank the EPSRC for funding on Grant Nos. EP/R003556/1 and EP/V00607X/1. E.J.S. acknowledges the support from the Australian Research Council Future Fellowship No. FT190100263, the National Health Medical Research Council Ideas Grant No. 2002510, and the Future Industries Accelerator Mobility Scheme MOB024.

DATA AVAILABILITY

The data that support the findings of this study are available within the article and its supplementary material.

REFERENCES

[1]J. Davies and D. Davies, Microbiol. Mol. Biol. Rev. **74**, 417–433 (2010).
[2]J. O'Neil, "Tackling drug-resistant infections globally: Final report and recommendations" (2016), see https://amr-review.org/sites/default/files/160518_Final%20paper_with%20cover.pdf.
[3]A. Khlyustova, C. Labay, Z. Machala, M. P. Ginebra, and C. Canal, Front. Chem. Sci. Eng. **13**, 238–252 (2019).
[4]T. Von Woedtke, S. Emmert, H. R. Metelmann, S. Rupf, and K. D. Weltmann, Phys. Plasmas **27**, 070601 (2020).
[5]B. Ghimire, E. J. Szili, P. Lamichhane, R. D. Short, J. S. Lim, P. Attri, K. Masur, K. D. Weltmann, S. H. Hong, and E. H. Choi, Appl. Phys. Lett. **114**, 093701 (2019).

[6]N. Gaur, E. J. Szili, J. S. Oh, S. H. Hong, A. Michelmore, D. B. Graves, A. Hatta, and R. D. Short, Appl. Phys. Lett. **107**, 103703 (2015).
[7]P. J. Bruggeman, M. J. Kushner, B. R. Locke, J. G. E. Gardeniers, W. G. Graham, D. B. Graves, R. C. H. M. Hofman-Caris, D. Maric, J. P. Reid, E. Ceriani, D. Fernandez Rivas, J. E. Foster, S. C. Garrick, Y. Gorbanev, S. Hamaguchi, F. Iza, H. Jablonowski, E. Klimova, J. Kolb, F. Krcma, P. Lukes, Z. MacHala, I. Marinov, D. Mariotti, S. Mededovic Thagard, D. Minakata, E. C. Neyts, J. Pawlat, Z. L. Petrovic, R. Pflieger, S. Reuter, D. C. Schram, S. Schröter, M. Shiraiwa, B. Tarabová, P. A. Tsai, J. R. R. Verlet, T. Von Woedtke, K. R. Wilson, K. Yasui, and G. Zvereva, Plasma Sources Sci. Technol. **25**, 053002 (2016).
[8]A. Barjasteh, Z. Dehghani, P. Lamichhane, N. Kaushik, and E. H. Choi, Appl. Sci. **11**, 3372 (2021).
[9]W. Tian and M. J. Kushner, J. Phys. D: Appl. Phys. **47**, 165201 (2014).
[10]S. Ikawa, K. Kitano, and S. Hamaguchi, Plasma Process. Polym. **7**, 33–42 (2010).
[11]S. Ikawa, A. Tani, Y. Nakashima, and K. Kitano, J. Phys. D: Appl. Phys. **49**, 425401 (2016).
[12]P. Lukes, E. Dolezalova, I. Sisrova, and M. Clupek, Plasma Sources Sci. Technol. **23**, 015019 (2014).
[13]H. J. Hathaway, B. L. Patenall, N. T. Thet, A. C. Sedgwick, G. T. Williams, A. T. A. Jenkins, S. L. Allinson, and R. D. Short, J. Phys. D: Appl. Phys. **52**, 505203 (2019).
[14]HERA, "Human & Environmental Risk Assessment on Ingredients of European Household Cleaning Products: Tetra acetyl ethylene diamine (TAED)," Report No. CAS 10543-57-4 (HERA, 2002).
[15]P. Sofokleous, S. Ali, P. Wilson, A. Buanz, S. Gaisford, D. Mistry, A. Fellows, and R. M. Day, Acta Biomater. **64**, 301–312 (2017).
[16]K. Liu, X. Zhang, and K. Yan, Cellulose **24**, 1555–1561 (2017).
[17]R. Warburton, *Peracetic Acid in the Fresh Food Industry* (Food Safety Magazine, 2014).
[18]M. Kitis, Environ. Int. **30**, 47–55 (2004).
[19]W. A. Rutala and D. J. Weber, *Disinfection, Sterilization and Control of Hospital Waste*, 8th ed. (Elsevier, 2015).
[20]B. Becker, F. H. H. Brill, D. Todt, E. Steinmann, J. Lenz, D. Paulmann, B. Bischoff, and J. Steinmann, Antimicrob. Resist. Infect. Control **6**, 1–6 (2017).
[21]B. Ghimire, E. J. Szili, B. L. Patenall, P. Lamichhane, N. Gaur, A. J. Robson, D. Trivedi, N. T. Thet, A. T. A. Jenkins, E. H. Choi, and R. D. Short, Plasma Sources Sci. Technol. **30**, 035009 (2021).
[22]B. Ghimire, J. Sornsakdanuphap, Y. J. Hong, H. S. Uhm, K. D. Weltmann, and E. H. Choi, Phys. Plasmas **24**, 073502 (2017).
[23]A. J. Wu, H. Zhang, X. D. Li, S. Y. Lu, C. M. Du, and J. H. Yan, IEEE Trans. Plasma Sci. **43**, 836–845 (2015).
[24]G. Jentsch, "Bacteriocidal washing agents contain. A per-compound and TAED:PAG mixture," US patent-US5021182A (1991), https://patents.google.-com/patent/US5021182A/en